

# The human reduced folate carrier gene is ubiquitously and differentially expressed in normal human tissues: identification of seven non-coding exons and characterization of a novel promoter

Johnathan R. WHETSTONE\*, Robin M. FLATLEY† and Larry H. MATHERLY\*†<sup>1</sup>

\*Department of Pharmacology, Barbara Ann Karmanos Cancer Institute, Wayne State University School of Medicine, Detroit, MI, U.S.A., and †Experimental and Clinical Therapeutics Program, Barbara Ann Karmanos Cancer Institute, Wayne State University School of Medicine, Detroit, MI, U.S.A.

Our previous study identified two alternate non-coding upstream exons (A and B) in the human reduced folate carrier (hRFC) gene, each controlled by a separate promoter. Each minimal promoter was regulated by unique *cis*-elements and transcription factors, including stimulating protein (Sp) 1 and Sp3 and the basic leucine zipper family of proteins, suggesting opportunities for cell- and tissue-specific regulation. Studies were performed to explore the expression patterns of hRFC in human tissues and cell lines. Levels of hRFC transcripts were measured on a multi-tissue mRNA array from 76 human tissues and tumour cell lines and on a multi-tissue Northern blot of representative tissues, each probed with full-length hRFC cDNA. hRFC transcripts were ubiquitously expressed, with the highest level in placenta and the lowest level in skeletal muscle. By rapid amplification of cDNA 5'-ends assay from nine tissues and two cell lines, hRFC transcripts containing both A and B 5'-untranslated regions

(UTRs) were identified. However, five additional 5'-UTRs (designated A1, A2, C, D and E) were detected, mapping over 35 kb upstream from the hRFC translation start site. The 5'-UTRs were characterized by multiple transcription start sites and/or alternative splice forms. At least 18 unique hRFC transcripts were detected. A novel promoter was localized to a 453 bp fragment, including 442 upstream of exon C and 11 bp of exon C. A 346 bp repressor flanked the 3'-end of this promoter. Our results suggest an intricate regulation of hRFC gene expression involving multiple promoters and non-coding exons. Moreover, they provide a transcriptional framework for understanding the role of hRFC in the pathophysiology of folate deficiency and antifolate drug selectivity.

**Key words:** alternative splicing, methotrexate, tissue-specificity, transcription.

## INTRODUCTION

Reduced folates are essential cofactors for the synthesis of DNA, RNA and amino acid precursors. Purines, thymidylate, serine and methionine are products of one-carbon transfer reactions from reduced folates in various anabolic pathways [1]. Since mammals lack the ability to synthesize reduced folates, cellular uptake of these derivatives is critical for cell growth and survival. A number of pathophysiological states are associated with folate deficiency, including cardiovascular disease [2], foetal abnormalities [3–7], neurological disorders [8] and cancer [9–11]. Although uptake of folates into mammalian cells and tissues can be mediated by the family of folate receptors or the reduced folate carrier (RFC), RFC is viewed as the primary route for membrane transport of reduced folate cofactors in mammalian cells [12–16].

RFC is also responsible for the cellular uptake of the first- and second-generation 'classical' antifolate cancer chemotherapeutic drugs, i.e. methotrexate (Mtx) and Tomudex [13–16]. Mtx remains the cornerstone in the modern treatment of childhood acute lymphoblastic leukaemia (ALL) and is a major agent used in the treatment of other malignancies, such as osteosarcoma [17,18]. Impaired Mtx transport results from sustained exposures of human and murine tumour cells to Mtx *in vitro* [19–23] and murine tumour cells *in vivo* after chemotherapy with Mtx [24].

Further, alterations in the levels and/or function of the human RFC (hRFC) were described in clinical specimens [18,25,26]. For instance, we previously reported an 88-fold range of hRFC expression in B-precursor ALL lymphoblasts and a proportional loss of Mtx transport capacity at low levels of hRFC [25]. Similarly, Guo et al. [18] showed that low levels of hRFC in osteosarcomas corresponded to decreased transport and a poor prognosis.

The critical role of reduced folate cofactors in normal tissue physiology implies that RFC is widely expressed and intricately regulated in response to cell- or tissue-specific stimuli. Recently, Wang et al. [27] demonstrated that murine RFC (mRFC) is expressed in a wide range of tissues by immunohistochemical detection with an mRFC-specific antibody; however, the site of mRFC expression (i.e. basolateral versus apical) was variable.

Our own studies suggested an important role for transcriptional controls as determinants of hRFC levels. Our laboratory demonstrated previously [28] that the hRFC gene is controlled by two functional GC-rich, TATA-less promoters that control transcription of two non-coding upstream exons (designated A and B), characterized by alternate transcription start sites and multiple splice forms. Although a similar upstream structure was reported by other laboratories [29–31], an additional putative non-coding exon approx. 1.7 kb upstream of exon B was described in one report [31]. For the hRFC promoter

Abbreviations used: ALL, acute lymphoblastic leukaemia; CRE, cAMP-response element; MTE, multi-tissue; MTN, 12-lane human multi-tissue Northern blot; Mtx, methotrexate; poly(A)<sup>+</sup>, polyadenylated; RACE, rapid amplification of cDNA ends; RFC, reduced folate carrier; hRFC, human RFC; mRFC, murine RFC; RT, reverse transcriptase; Sp, stimulating protein; 5'-UTR, 5'-untranslated region.

<sup>1</sup> To whom correspondence should be addressed at the Experimental and Clinical Therapeutics Program (e-mail matherly@karmanos.org).

The nucleotide sequences reported in this study will appear in GenBank® and EMBL databases with accession nos. AY089985, AY089986, AY089987 and AY089988.

B, important roles for stimulating protein (Sp) 1 and Sp3 were suggested for HT1080 and HepG2 cells [32]; the minimal A promoter was regulated by a cAMP-response element (CRE)/activator protein 1 ('API')-like element that interacted with diverse basic leucine zipper DNA-binding proteins, including CRE-binding protein ('CREB')-1, activating transcription factor ('ATF') 1 and c-Jun [32].

The pattern of promoter and exon utilization in assorted cells and tissues is probably the result of multiple transcription factors and/or epigenetic events that are able to respond to specific stimuli and ensure sufficient hRFC levels for cell proliferation and tissue regeneration. This may also contribute to the up-regulation of RFC expression and transport in a variety of cell lines grown in folate-restrictive environments [33–36], which may parallel molecular events occurring in specific tissues. On this basis, we initiated a systematic analysis of hRFC expression and promoter usage in human tissues. Our results demonstrate that hRFC is ubiquitously expressed. Whereas transcripts originating from both hRFC-A and -B non-coding exons were confirmed in normal tissues and tumour cell lines by 5'-rapid amplification of cDNA ends (5'-RACE) and/or reverse transcriptase (RT)-PCR analysis, five additional 5'-non-coding exons (designated A1, A2, C, D and E) were also detected. These results provide a transcriptional framework in understanding the role of hRFC in the pathophysiology associated with folate deficiency and antifolate selectivity during chemotherapy.

## MATERIALS AND METHODS

### Chemicals and reagents

[ $\alpha$ -<sup>32</sup>P]dCTP (3000 Ci/mmol) was purchased from PerkinElmer (Boston, MA, U.S.A.). Synthetic oligonucleotides were obtained from Genosys Biotechnologies (The Woodlands, TX, U.S.A.). Lipofectin® was purchased from Life Technologies (Bethesda, MD, U.S.A.). Restriction and modifying enzymes, reporter gene vectors (pGL3-Basic, pGL3 Pro and pRLSV40) and other molecular materials were obtained from Promega (Madison, WI, U.S.A.).

### Cell culture

The HT1080 human fibrosarcoma, HepG2 human hepatoma, K562 erythroleukaemia, REH B-precursor ALL, Molt 3 T-ALL and Daudi B lymphoma cell lines were all obtained from A.T.C.C. (Rockville, MD, U.S.A.). Nalm 6 cells were obtained from DSMZ (German Collection of Microorganisms and Cell Culture, Braunschweig, Germany). CCRF-CEM and Jurkat T-ALL cells were gifts from Dr Andre Rosowsky (Boston, MA, U.S.A.) and Dr Beverly Mitchell (Chapel Hill, NC, U.S.A.) respectively. HepG2 cells were cultured in minimum essential medium supplemented with 10% foetal bovine serum and antibiotics at 37 °C. The other cell lines were grown in RPMI 1640 medium with 10% heat-inactivated iron-supplemented calf serum (Hyclone Labs, Logan, UT, U.S.A.), 2 mM L-glutamine, 100 units/ml penicillin and 100 µg/ml streptomycin, in a 5% CO<sub>2</sub>/95% air atmosphere at 37 °C. K562.4CF cells were derived in this laboratory from parental K562 cells by selection with 0.4 nM (6*R,S*)5-formyl tetrahydrofolate as the sole folate source [33]. These cells were maintained as described previously [33].

### Northern-blot analysis

A multi-tissue (MTE) array containing 76 different polyadenylated [poly(A)<sup>+</sup>] RNAs from human tissues and tumour cell lines and a 12-lane human multi-tissue Northern blot (MTN)

**Table 1** Positions of the hRFC non-coding exons and first coding exon

Exon	Position*
1	236798–237039
A1	236799–237039
A2	237552–237818
A	240254–240655
B	241064–241222
C	242936–243515
D	260815–261280
E	271314–271555

\* The numbering corresponds to chromosome 21 contig HS21C102 (accession no. AL163302).

were purchased from ClonTech Laboratories (Palo Alto, CA, U.S.A.). Blots were hybridized with <sup>32</sup>P-labelled full-length hRFC cDNA, labelled by random priming (Roche, Indianapolis, IN, U.S.A.) and purified on a Sephadex G-25 column [37]. Hybridization and washes were performed according to the manufacturer's instructions. After several washes, the membranes were exposed to X-ray film. Densitometry for the MTE array was conducted on a PhosphorImager (Molecular Dynamics, Sunnyvale, CA, U.S.A.) and analysed using ImageQuant software (Molecular Dynamics). The values were expressed in arbitrary units after subtracting the dot background.

### 5'-RACE assay

Trizol reagent (Gibco BRL, Gaithersburg, MD, U.S.A.) was used to isolate total RNA from HT1080 and HepG2 cells. mRNA for each cell line was purified from the total RNA, using the Oligotex mRNA Midi kit from Qiagen. Poly(A)<sup>+</sup> RNAs for assorted human tissues were purchased from ClonTech Laboratories. Poly(A)<sup>+</sup> RNAs were analysed by 5'-RACE using the Marathon cDNA amplification kit (ClonTech Laboratories) [28]. 5'-RACE products were subcloned into pGEM-T Easy vector (Promega) and 15–28 5'-RACE clones were sequenced by automated sequencing for each tissue/cell line, using the RFCN-1 antisense primer (5'-AGCTCCGGAGGGGACGAA-GGTGACACTGTG-3'). The 5'-untranslated regions (UTRs) were mapped to non-coding exons on chromosome 21 contig HS21C102 (accession no. AL163302) and numbered accordingly, where the hRFC ATG start site is position 236749 (see Table 1). The nucleotide sequence for each novel non-coding exon has been submitted to GenBank® under the following accession numbers: AY089985 for exons A1/A2, AY089988 for exon C, AY089986 for exon D and AY089987 for exon E.

### RT-PCR analysis of 5'-non-coding hRFC exons

To confirm non-coding exon sequences in hRFC transcripts, poly(A)<sup>+</sup> mRNAs from human tissues and total RNAs from multiple cell lines were reverse transcribed with random hexamers and an RT-PCR kit (PerkinElmer). The cDNAs were amplified with exon-specific upstream primers for exons A1 [RT-PCR A1 (5'-TCAGCCTCGGAGACCCTGGAGTGGTGAC-3')], A2 [RT-PCR A2 (5'-CGCCCTCGAGTGTGCTTCGTGCTGCTGCTG-3')], A [KS32-300U A (5'-TGTCATCGGAAACTC-CTGTC-3')], B [KS43-45U B (5'-CGAGTCGCAGGCACAGTGTCA-3')], C [RT-PCR C (5'-GGCCTTGTGTGCTGGGAACTCCCAGGACTC-3')], D [RT-PCR D (5'-TGTTGGAATCTACGTAAATTCAGCTCCT-3')] and E [RT-PCR E1 (5'-CTACCCCAGGTTGTCTCTTCGTGGGAA-3')], and a

universal downstream primer in the hRFC coding region [KS43-323L (5'-TACTCCTACCTGGCCGTGCTGG-3')] for all exons except exon A, which used KS32-774 (5'-TTCTACAGCGT-CACCATGGC-3'). For exons A1, A2, A, B, C and D, a single PCR amplification was used. PCR conditions for exons A1 and A2 were 94 °C for 5 min (1 cycle); 94 °C for 15 s, 60 °C for 45 s and 72 °C for 45 s (40 cycles); and 72 °C for 7 min (1 cycle). For exons A, B, C and D, PCR conditions were 94 °C for 5 min (1 cycle); 94 °C for 15 s, 63 °C for 45 s and 72 °C for 45 s (35 cycles); and 72 °C for 7 min (1 cycle). For exon E, two amplifications were used. These include a primary reaction with RT-PCR E1 and KS43-323L primers at 94 °C for 5 min (1 cycle); 94 °C for 15 s, 65 °C for 45 s and 72 °C for 45 s (35 cycles); and 72 °C for 7 min (1 cycle). A secondary amplification (on 50-fold diluted primary product) was performed with a nested exon E primer [RT-PCR E2 (5'-CGCGTGAAGCT-TGCCCTCTGTAAGCCTGT-3')] and KS43-323L, using the same conditions. The PCR amplification for the coding region of hRFC used P8 (5'-CAGTGTACCTTCGTCCCCTCCG-3') and P7 (5'-GCCAGCGAGATGTAGTTGAGCGT-3') primers and the same conditions as for exons A, B, C and D, except that only 33 cycles were used. The 18 S RNAs were amplified with commercial primers (Ambion, Austin, TX, U.S.A.) with the same conditions as for exons A1 and A2, except that 25 cycles were used. PCR products were electrophoresed on a 2% LE agarose gel with ethidium bromide, and the amplicons were isolated from the gel with the Concert Rapid Gel Extraction Kit (Gibco BRL). Sequences for the PCR products were obtained by automated DNA sequencing.

#### Primer extension analysis

Primer extension was used to confirm 5'-ends as described previously by Zhang et al. [28].

#### hRFC-luciferase reporter constructs

A genomic fragment of RFCg1-3d [28] was digested with *KpnI* to generate a 2883 bp fragment of chromosome 21 sequence, including exon C and both 5'- and 3'-flanking regions (GenBank® accession no. AY089988). This fragment was subcloned into pGL3-Basic in the sense direction (hRFC-C/2883). 5'- and 3'-deletions were introduced into the hRFC-C/2883 reporter construct with restriction endonucleases including *SanDI*, *BsmBI* and *PstI* (5'-deletions) and *NcoI* and *BstAPI* (3'-deletions). PCR was also used to make a 5'-deletion (hRFC-C/151) using the ProC Del3 (5'-ACTGCCTCGAGCACTGTCTGTGGCCACT-CCTCGCAGTCCTC-3') and ProC (BstapI) *HindIII* (5'-CTAGCTAAGCTTCTGCTTCGGAGTGGGGAGGTAGGGC-TTCT-3') primers with the following PCR conditions: 94 °C for 5 min (1 cycle); 94 °C for 15 s, 65 °C for 45 s and 72 °C for 45 s (40 cycles); and 72 °C for 7 min (1 cycle). This amplicon was digested with *XhoI*-*HindIII* and subcloned into the multiple-cloning site of pGL3-Basic.

#### Transient transfections and reporter gene assays

HepG2 cells were seeded at  $1 \times 10^5$  cells/well in 6-well dishes 24 h before transfection. The plates used for HepG2 cells were coated with 4 µg/ml poly-L-lysine. hRFC-C promoter constructs or empty pGL3-basic vector (475 ng) were co-transfected with 25 ng of pRLSV40 plasmid, using 3 µg Lipofectin® according to the manufacturer's instructions [32]. After 24 h, the cells were washed and media was added. After an additional 48 h, lysates were prepared and firefly luciferase activity was assayed using the Dual Luciferase Kit (Promega) in a Turner 20/20 luminometer.

Firefly luciferase activity was normalized with *Renilla* luciferase. For all transfections, three or more experiments were performed in duplicate.

## RESULTS

### The hRFC gene is ubiquitously and differentially expressed in human tissues and tumours

Experiments were performed to assess the global expression patterns of the hRFC gene in human tissues and tumours. An MTE array containing mRNAs from 68 human tissues and eight tumour cell lines was hybridized with the full-length hRFC cDNA (Figure 1A). hRFC transcripts were detected in all tissues, although at variable levels. The range of expression was 12-fold. For the adult tissues, placenta (B8) had the highest hRFC level, followed by the liver (A9) and peripheral blood leucocytes (E7), with very low levels in the heart (A4) and skeletal muscle (B7). The central nervous system and brain had relatively high levels of hRFC transcripts, with the highest levels in the caudate nucleus (E2) and cerebellum (A2, B2) (Figure 1A). Of the tumour cell lines analysed for hRFC expression, the highest levels of transcripts were detected in K562 cells (C10). Differential hRFC expression was also observed with the human foetal tissues (lanes A11–G11), with the highest level in foetal lung (G11) and the lowest level in foetal heart (B11). The hRFC cDNA did not hybridize with the majority of the negative controls in lane 12; however, the cDNA probe did hybridize with *Escherichia coli* rRNA (C12) and *E. coli* DNA (D12). This may reflect either sequence homologies with *E. coli* genes or, most likely, non-specific hybridization.

The MTE array results were further confirmed on an MTN hybridized with the full-length hRFC cDNA. All tissues expressed a primary, approx. 3.1 kb, transcript, although additional larger or smaller transcript forms were detected, presumably due to the variable polyadenylation and/or alternative splicing (Figure 1B). Although minor differences were observed between hRFC transcript levels in tissues on the MTN when compared with the same tissues on the MTE array, the major patterns were, nonetheless, preserved, with the highest levels in the liver and placenta and the lowest levels in skeletal muscle and heart (Figure 1B). Thus the MTN results validate the hRFC expression patterns observed on the MTE array. Overall, these results demonstrate that the hRFC gene is ubiquitously and differentially expressed in human tissues.

### 5'-UTRs in hRFC transcripts are expressed in a tissue-specific manner

Previous studies on the upstream region of the hRFC gene [28–31] confirmed that 5'-UTR heterogeneity in hRFC transcripts arose from up to three non-coding exons that variably splice but fuse to a common coding exon (exon 1) at position 236798 (in chromosome 21 contig HS21C102; equivalent to position 49, where the translation start is 0). Exons B and A are transcribed from separate promoters (promoters B and A respectively). Tissue differences in the regulation and utilization of alternate promoters and their respective transcripts could account for the different levels of hRFC transcripts observed in the assortment of human tissues in Figure 1.

5'-RACE was used to extend our studies of hRFC expression patterns to human tissues by determining 5'-UTR and promoter usage for select tissues, including caudate nucleus (E2 in Figure 1A), lung (A8), foetal lung (G11), liver (A9), foetal liver (D11), bone marrow (G7), small intestine (C5–F5), heart (A4) and placenta (B8). Based on our previous studies of hRFC promoter

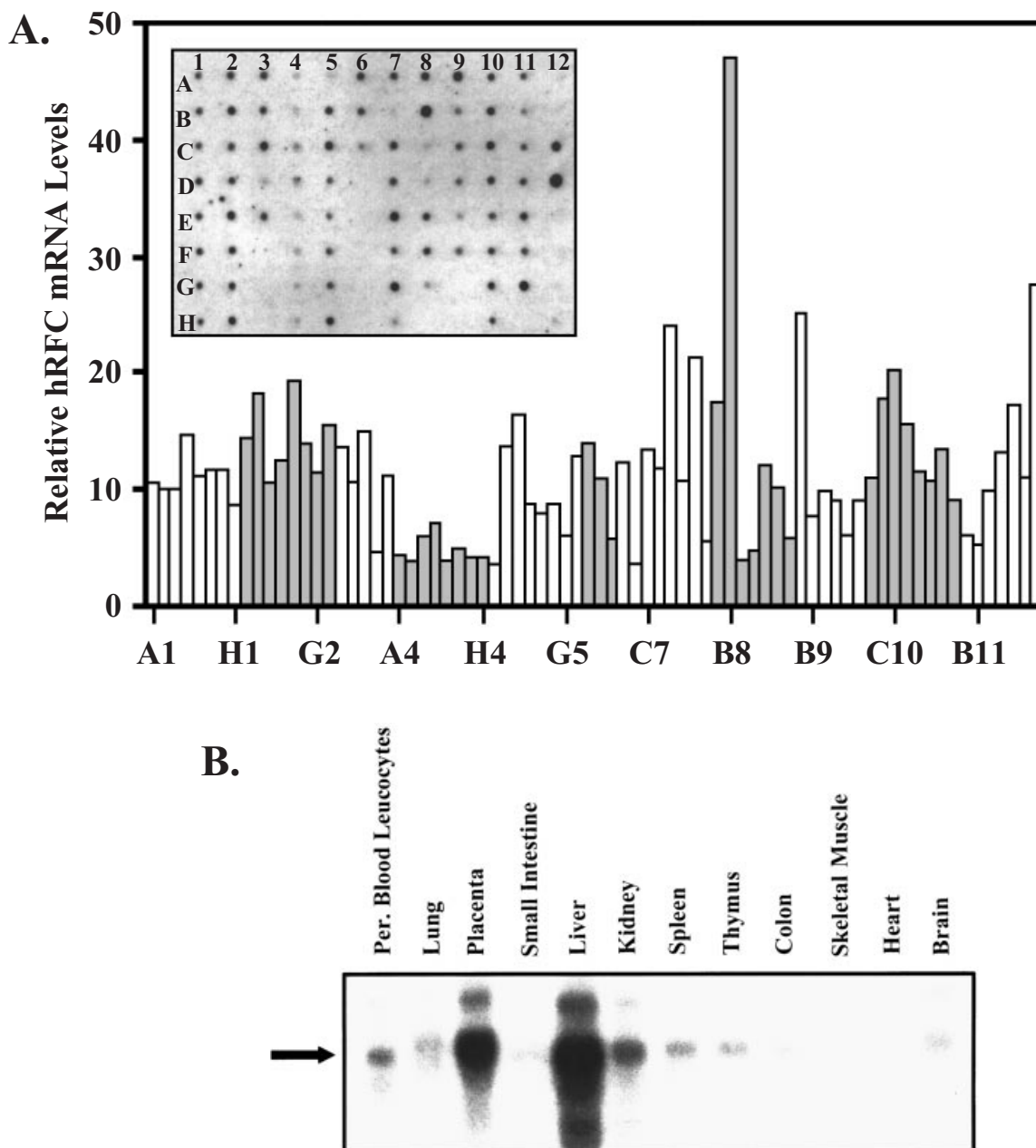


**Figure 1** hRFC mRNA levels in human tissues and cell lines

(A) An MTE array was hybridized with a  $^{32}\text{P}$ -labelled hRFC cDNA. The relative intensities of the signals from the MTE array (inset) minus background from an area without sample were plotted. The  $x$ -coordinates on the graph correspond to those on the MTE array and are given sequentially: A1, whole brain; B1, cerebral cortex; C1, frontal lobe; D1, parietal lobe; E1, occipital lobe; F1, temporal lobe; G1, paracentral gyrus of cerebral cortex; H1, pons; A2, cerebellum, left; B2, cerebellum, right; C2, corpus callosum; D2, amygdala; E2, caudate nucleus; F2, hippocampus; G2, medulla oblongata; H2, putamen; A3, substantia nigra; B3, accumbens nucleus; C3, thalamus; D3, pituitary gland; E3, spinal cord; A4, heart; B4, aorta; C4, atrium, left; D4, atrium, right; E4, ventricle, left; F4, ventricle, right; G4, interventricular septum; H4, apex of heart; A5, oesophagus; B5, stomach; C5, duodenum; D5, jejunum; E5, ileum; F5, ilocaecum; G5, appendix; H5, colon, ascending; A6, colon, transverse; B6, colon, descending; C6, rectum; A7, kidney; B7, skeletal muscle; C7, spleen; D7, thymus; E7, peripheral blood leucocyte; F7, lymph node; G7, bone marrow; H7, trachea; A8, lung; B8, placenta; C8, bladder; D8, uterus; E8, prostate; F8, testis; G8, ovary; A9, liver; B9, pancreas; C9, adrenal gland; D9, thyroid gland; E9, salivary gland; F9, mammary gland; A10, HL-60 cells; B10, HeLa S3 cells; C10, K-562 cells; D10, MOLT-4 cells; E10, Raji cells; F10, Daudi cells; G10, SW480 cells; H10, A549 cells; A11, foetal brain; B11, foetal heart; C11, foetal kidney; D11, foetal liver; E11, foetal spleen; F11, foetal thymus; G11, foetal lung; A12, yeast total RNA; B12, yeast tRNA; C12, *E. coli* rRNA; D12, *E. coli* DNA; E12, Poly r(A); F12, human  $\text{C}_\theta$ -1 DNA; G12, human DNA (100 ng); H12, human DNA (500 ng). (B) An MTN blot was hybridized with the  $^{32}\text{P}$ -labelled hRFC cDNA and exposed to X-ray film, as described in the Materials and methods section.

structure and function in HT1080 fibrosarcoma and HepG2 hepatoma cells [28,32], 5'-RACE assays were also performed with mRNAs from these cell lines. HT1080 and HepG2 cells express moderate to high levels of hRFC transcripts (J. R. Whetstine and L. H. Matherly, unpublished work).

Double-stranded cDNA templates were prepared from poly(A)<sup>+</sup> mRNAs from the tissues and cell lines and ligated to anchor adapters. After PCR amplification with nested anchor primers (anchor primers 1/2) and gene-specific primers (RFCo-1/RFCN-1), the amplicons were ligated into pGEM-T easy

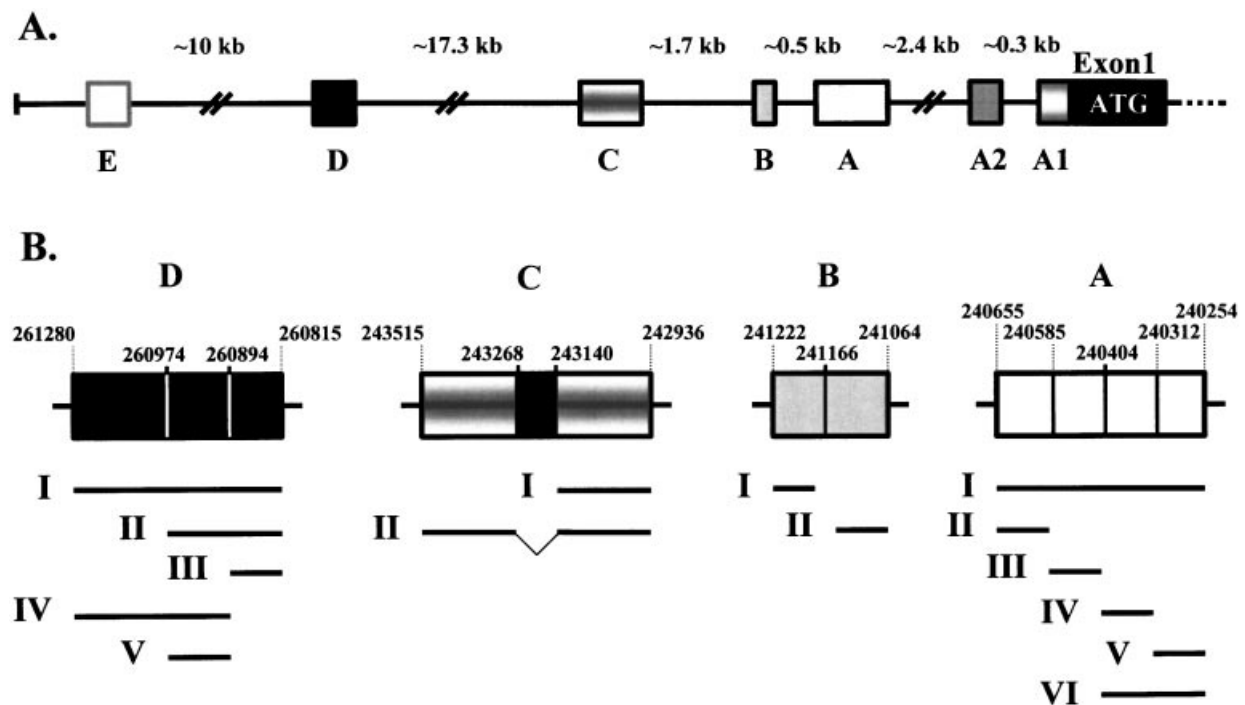


**Figure 2** Schematic representation of hRFC non-coding exons and their representative splice forms

(A) The upstream region of the hRFC gene including seven non-coding exons (A1, A2 and A–E) and the first coding exon (Exon 1) including the ATG translation start site. The approximate distances between each of the non-coding exons were determined from those in chromosome 21 contig HS21C102 (accession no. AL163302). (B) The putative alternate splice forms for non-coding exons D, C, B and A are depicted, as described in the Results section. The numbering corresponds to positions on contig HS21C102. From the analysis of sequence patterns in 5'-RACE clones from multiple tissues and cell lines, five putative splice forms were identified for exon D, two for exons C and B and six for exon A.

**Table 2** Distribution of non-coding exons and splice forms in human tissues and cell lines

The data summarize the distributions of 5'-RACE clones from tissues and cell lines as described in the Results section. Ratios refer to the numbers of 5'-RACE clones for a particular exon (A–D, A1, A2 and E) including all splice forms to the total clones analysed (all exons) for a particular tissue or cell line.

Tissues	Exon A							Exon B			Exon C			Exon D					Exon A1 (Ratio)	Exon A2 (Ratio)	Exon E (Ratio)	
	AI	AII	AIII	AIV	AV	AVI	Ratio	BI	BII	Ratio	CI	CII	Ratio	DI	DII	DIII	DIV	DV				Ratio
Lung	0	0	0	0	0	0	0/18	0	0	0/18	1	0	1/18	7	2	6	0	0	15/18	1/18	0/18	1/18
Foetal lung	0	0	0	0	0	0	0/19	0	0	0/19	0	2	2/19	3	7	6	1	0	17/19	0/19	0/19	0/19
Liver	0	0	2	2	2	2	8/16	1	0	1/16	0	0	0/16	0	0	0	0	0	0/16	0/16	7/16	0/16
Foetal liver	1	6	0	0	7	1	15/16	0	0	0/16	0	0	0/16	0	0	0	0	0	0/16	1/16	0/16	0/16
Heart	0	0	0	0	0	0	0/15	9	0	9/15	0	0	0/15	0	0	0	0	0	0/15	6/15	0/15	0/15
Caudate nucleus	0	0	0	0	0	0	0/27	0	0	0/27	3	5	8/27	5	12	1	0	1	19/27	0/27	0/27	0/27
Bone marrow	0	0	3	1	0	7	11/19	2	0	2/19	5	0	5/19	0	0	0	0	0	0/19	1/19	0/19	0/19
Placenta	0	0	0	0	0	0	0/20	2	1	3/20	17	0	17/20	0	0	0	0	0	0/20	0/20	0/20	0/20
Small intestine	0	0	0	0	0	1	1/19	0	0	0/19	0	0	0/19	4	14	0	0	0	18/19	0/19	0/19	0/19
HT1080	4	3	0	0	0	0	7/19	10	2	12/19	0	0	0/19	0	0	0	0	0	0/19	0/19	0/19	0/19
HepG2	2	6	4	0	0	1	13/19	4	1	5/19	1	0	1/19	0	0	0	0	0	0/19	0/19	0/19	0/19

plasmid for transformation and sequencing. 5'-RACE clones (15–28) were sequenced for each tissue/cell line and the sequences were aligned with contig HS21C102 (Table 1).

A total of seven putative non-coding exons were identified by 5'-RACE, including those originating from non-coding exons B and A. When these non-coding exon sequences were aligned with contig HS21C102, they localized to within approx. 35 kb upstream from the ATG start site in exon 1 (Figure 2A; Table 1). Exon A1 was immediately juxtaposed 5' to the first coding exon (exon 1) and was followed in succession by exons A2, A, B, C, D

and, finally, E (Figure 2A; Table 1). Exon C appears to be identical with a putative hRFC non-coding exon reported to map approx. 1.7 kb upstream from exon B [31].

The distributions of 5'-UTRs were relatively tissue-specific (Table 2); however, the exon junctions were conserved between tissues expressing a particular 5'-UTR. In caudate nucleus, lung and foetal lung, exon D transcripts were the predominant forms detected, with lower levels of exon C. Exon D was, likewise, the major transcript form identified in small intestine; however, this was accompanied by exon A. RACE clones with 5'-UTRs from



**Figure 3** DNA sequences for hRFC 5'-UTRs

5'-RACE was performed as described in the Materials and methods section. Sequence data are shown for the seven unique 5'-UTRs (A1, A2 and A-E), and for exons A-D, the putative alternative splice forms. The numbering of each exon (or splice form) is based on that of contig HS21C102 and the sequence is shown in the sense direction. The circles represent probable transcription start sites for each of the 5'-UTRs. For exon A1, both non-coding exon and common exon 1 sequences are shown (the latter as lower-case letters and beginning at position 236798). Sequences A1 and D1 represent the full-length exons A and D respectively. Exon B comprises B1 and BII (these splice forms overlap at the AG). For forms A1 and B1, the 5'-ends are based on CCRF-CEM cells as described previously in [28]. Exon C encodes two splice forms, including C1 and CII. The various splice forms for exons A-D are indicated by normal, italicized, bold and/or underlined upper-case letters for clarity.

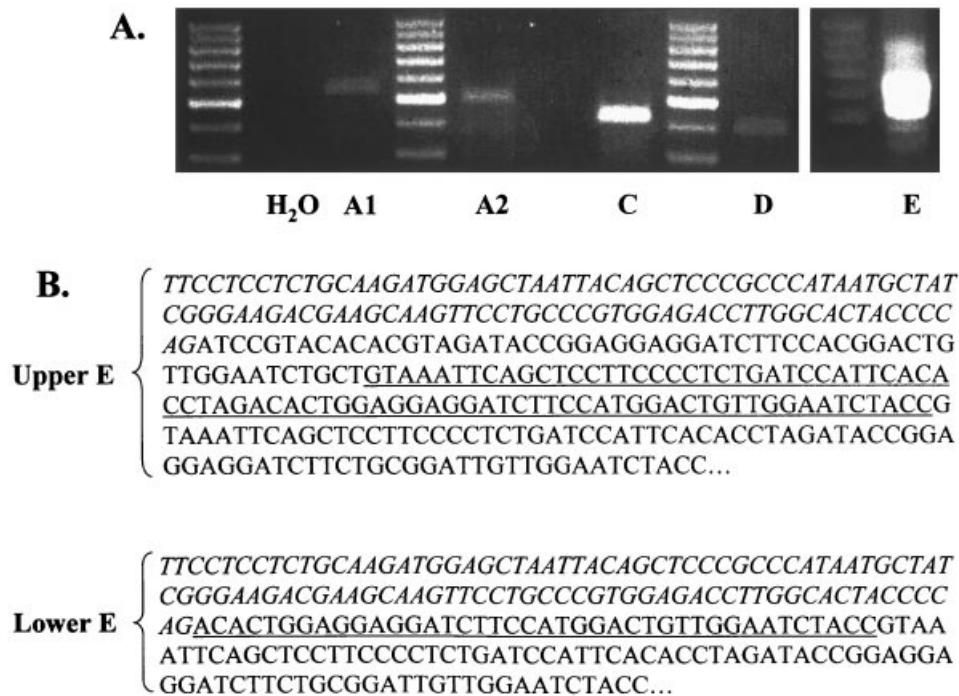


**Figure 4** Confirmation of novel 5'-UTRs in human tissues by RT-PCR

Poly(A)<sup>+</sup> mRNA from various tissues or cell lines were reverse transcribed and the cDNAs were amplified with sense primers specific to the individual non-coding exons and antisense primers to hRFC coding sequence (see the Materials and methods section). (A) A 2% agarose gel was used to separate the five novel non-coding exon amplicons including A1 (amplified from foetal liver), A2 (adult liver), C (placenta), D (lung) and E (lung). Each PCR product was verified by automated sequencing. (B) DNA sequence data for the two major PCR products for Exon E (A) are shown as described in the Results section. The italicized sequence represents exon E (from positions 271413 to 271314) and the non-italicized sequence is non-coding exon D from positions 261030 to 260815 (Upper E) and 260934 to 260815 (Lower E). The underlined sequence denotes the first of two identical 80 bp repeats in exon D.

exon A were the major forms identified in foetal liver, liver and bone marrow, with fewer clones derived from exons B (liver and bone marrow), A2 (liver), A1 (foetal liver and bone marrow) and C (bone marrow). In heart, 60% of the 5'-RACE clones contained exon B sequence and the remainder exon A1; in placenta, 17 of the 20 5'-RACE products contained exon C sequence and three were from exon B.

Apparent alternative splice forms were detected for four of the seven putative non-coding exons (Figures 2B and 3), including six for exon A (designated A1–AVI), two for exon B (BI and BII), two for exon C (CI and CII) and five for exon D (DI–DV; Figure 2B; Table 2). Conserved splice donor (GT) and acceptor (AG) elements invariably occurred in the deleted segments. There was no evidence for alternative splicing with transcripts containing 5'-UTRs derived from exons A1, A2 and E by 5'-RACE. Altogether, a total of 18 potential hRFC transcript forms were detected by 5'-RACE (Figure 2B). Figure 3 shows the DNA sequences for the major groups of 5'-RACE products, including the apparent splice forms derived from exons A–D.

Although most of the 5'-UTR splice forms were detected in more than one tissue, tissue-specific patterns were, nonetheless, apparent (Table 2). This is best exemplified by exon A for which liver expressed variants AIII–AVI, whereas bone marrow expressed the forms AIII, AIV and AVI. For exon B, form BII (previously KS6; [37]) was detected in placenta; however, this form was not detected in heart, bone marrow or adult liver (Table 2). Differences in 5'-UTRs and splice forms were, likewise, detected between foetal and adult tissues. For instance, 15 of the 16 5'-RACE clones from foetal liver were from exon A (A1, AII, AV and AVI splice forms), with a single A1 clone. For adult

liver, eight of the 16 5'-RACE products were from exon A (splice forms AIII–AVI), seven from A2 and one from BI (Table 2).

#### Confirmation of alternative 5'-UTRs in human tissues and cell lines by RT-PCR

RT-PCR was used to confirm the presence of the seven unique 5'-UTRs identified by 5'-RACE in hRFC transcripts. mRNAs from individual tissues or cell lines found to express particular 5'-UTRs by 5'-RACE were reverse-transcribed and amplified with 5'-UTR-specific primers and downstream primers in the hRFC coding region. For the A1, A2, C and D primers, a single amplification generated amplicons of the expected sizes that, upon sequencing, mapped to the hRFC upstream regions (Figure 4A). Since no specific product from exon E was detected after a single amplification of lung cDNAs, a secondary amplification was used to increase the sensitivity. Again, no product of the expected size was detected; rather, two products (316 and 220 bp) were identified (Figure 4A). Upon sequencing, these were found to contain overlapping 120 or 216 bp segments derived from exon D, including one or two 80 bp repeats, and linked to an identical 100 bp exon E fragment (Figure 4B).

The presence of these alternate hRFC non-coding exons was further confirmed in leukaemia and lymphoma cell line models by RT-PCR (Figure 5). In this analysis, hRFC transcripts with exons A1, B and C were frequent. Although exon D was not detected by primary PCR in any of the cell lines, this form was detected in Jurkat cells by secondary PCR with nested primers (results not shown). Exons A and E were less frequently detected; however, for exon A, this reflects the occurrence of

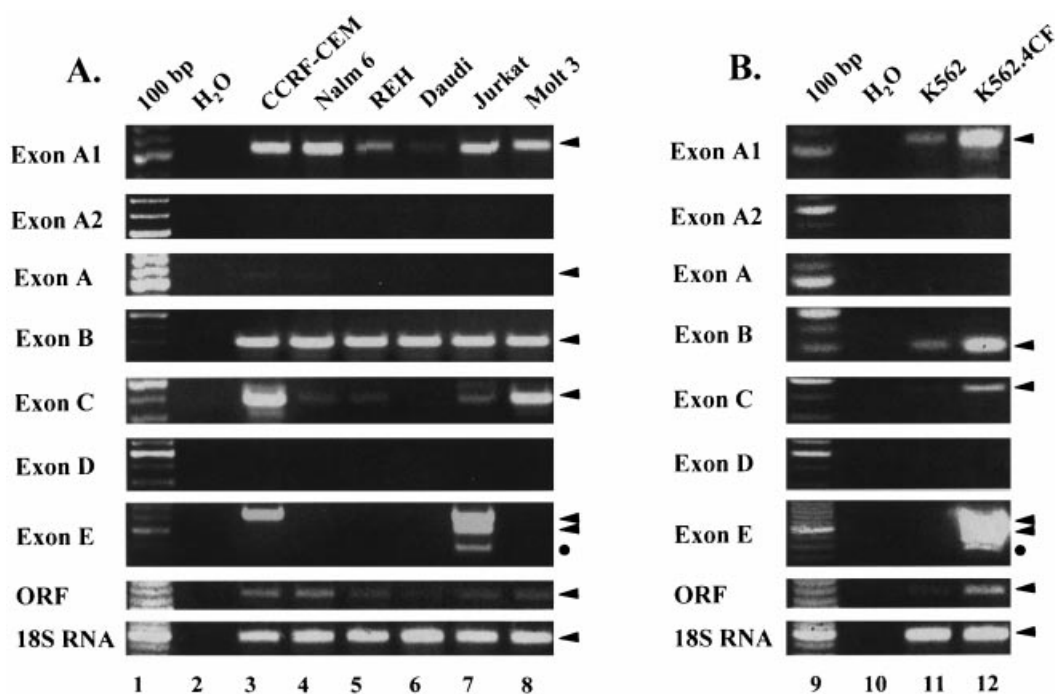


**Figure 5** Confirmation of 5'-UTRs in cell lines by RT-PCR

Total RNAs from various cell lines were reverse-transcribed and the cDNAs were amplified with sense primers specific to the individual non-coding exons and antisense primers to hRFC coding sequence (see the Materials and methods section). Total hRFC transcripts were detected with primers to the hRFC open reading frame (ORF), and 18 S RNAs were detected with commercial primers. (A, B) Results are shown for CCRF-CEM (lane 3), Nalm 6 (lane 4), REH (lane 5), Daudi (lane 6), Jurkat (lane 7), Molt 3 (lane 8), K562 (lane 11) and K562.4CF (lane 12) cells, after separation of the amplicons on a 2% agarose gel. Specific amplification products, as determined by DNA sequencing, are indicated by arrow heads, whereas non-specific products are indicated by circles. In lanes 2 and 10, negative control amplifications were made with RT reactions without RNA.

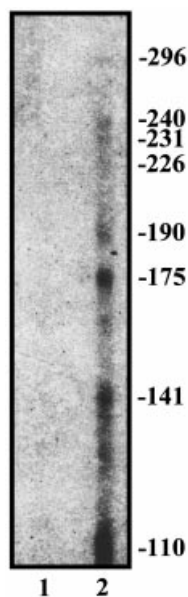


**Figure 6** Primer extension of K562.4CF total RNA

The RFCN-1 primer was  $^{32}\text{P}$ -end-labelled and annealed with no RNA (lane 1) or 100  $\mu\text{g}$  of total RNA from K562.4CF cells (lane 2). The extension products were analysed on a 6% denaturing polyacrylamide gel and the sizes were determined from adjacent sequencing reactions.

alternative splice forms not amplified with the 300/774 primer pair, since additional hRFC-A 5'-UTRs were detected with other primer pairs (results not shown). Exon A2 was not detected. Exon E could only be detected by secondary PCR and, again, all the transcripts were D and E hybrids. In Jurkat cells, both the 220 and 316 bp D and E products were detected, whereas in CCRF-CEM cells the 316 bp species was identified. RT-PCR also confirmed expression of hRFC in each of the cell lines tested.

Our experiments were extended to include 5'-UTR usage in K562.4CF cells, which were selected for growth under folate-restricted conditions (0.4 nM leucovorin), and exhibit approx. 4-fold increase in hRFC transcripts and approx. 6-fold increase in hRFC protein and Mtx transport [33,38]. In K562.4CF and parental K562 cells, hRFC transcripts containing exons A1, B, C and E were detected (Figure 5B). Notably, the increase in hRFC transcripts in K562.4CF cells was accompanied by an increase in non-coding exons (A1, B, C and E). Collectively, our RT-PCR results in primary human tissues and cell lines confirm the presence of seven unique 5'-UTRs for hRFC transcripts.

#### Identification of upstream transcriptional start sites in K562.4CF cells

Potential transcriptional start sites originating from the novel hRFC 5'-UTRs were mapped by primer extension analysis using template from 100  $\mu\text{g}$  of total RNA from K562.4CF cells. These

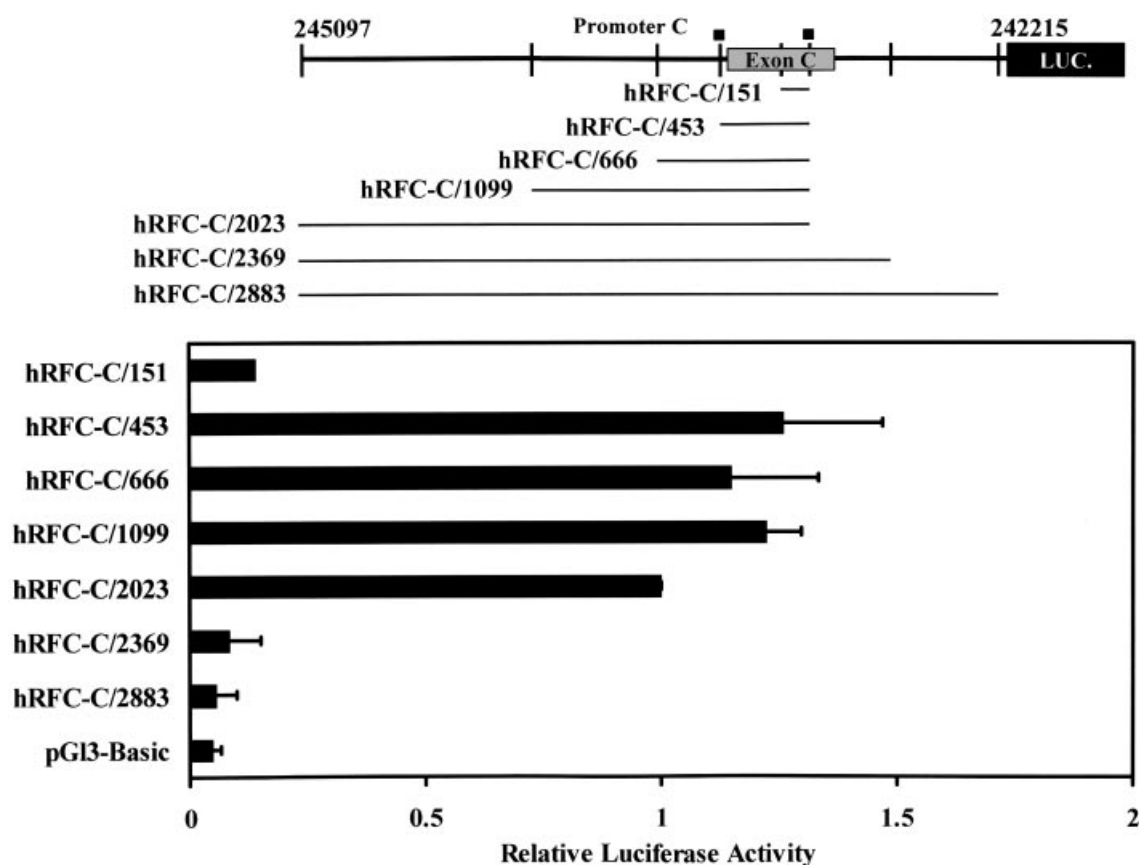


**Figure 7** Deletion analysis of hRFC-C promoter activity of hRFC gene in HepG2 cells

5'- and 3'-deletions were introduced into a 2883 bp fragment including 580 bp of exon C, as described in the Materials and methods section. Promoter constructs in pGL3-Basic were transiently expressed in HepG2 cells for luciferase reporter gene assays. Results are presented as relative firefly luciferase activities, normalized to *Renilla* luciferase activities. S.E.M. are shown by the error bars. In the upper schematic, ■ represents positions 243526–243074 corresponding to the DNA sequence for promoter C in Figure 8.

experiments were similar to those described previously by Zhang et al. [28]; however, the focus was on extension products larger than 110 bp. These products could conceivably represent transcripts with 5'-UTRs derived from exons A1, A2, A and C. As shown in Figure 6, extension products were detected from 110 to 296 bp, which was consistent with the transcriptional initiation sites for these cells and the predicted 5'-RACE products shown in Figure 3.

#### Exon C is transcribed by a novel promoter

By analogy with exons A and B, the 5'-flanking regions proximal to the novel A1, A2, C, D and E exons may each represent unique promoters. Since HepG2 cells use non-coding exon C (Table 2), these cells should be suitable for assaying the putative promoter C for activity, thus permitting the identification of important regulatory regions. A 2883 bp fragment of chromosome 21 (positions 245097–242215), including the 580 bp exon C, was isolated from an hRFC genomic clone and subcloned into the pGL3-Basic vector for transient transfection into HepG2 cells (Figure 7). At position 243265, a transition mutation (G to A) was observed in our clone when compared with the chromosome 21 contig. Therefore this nucleotide has been changed in our sequence to reflect our construct.

Promoter activity was negligible until a 346 bp fragment,

including 138 bp from the 3'-end of exon C, was removed (hRFC-C/2023; Figure 7). This suggests the presence of a strong repressor in this region (positions 243073–242728). However, this effect appeared to be specific to promoter C, since there was no effect on the SV40 basal promoter when the 346 bp fragment was subcloned into pGL3 Pro and assayed for promoter activity (results not shown). Thus the 346 bp downstream fragment does not appear to be a global silencer.

A series of 5'-deletions were constructed to evaluate possible regulatory regions in promoter C. Promoter activity was unaffected by progressive 5'-deletions, spanning 1573 bp, leaving 453 bp and including 11 bp of exon C (hRFC-C/453; Figure 7). When an additional 303 bp was deleted (i.e. hRFC-C/151), promoter activity was lost, indicating that the basal regulatory elements that co-ordinate the transcription for promoter C must be localized within this region. The promoter activity of the 453 bp region was orientation dependent, since activity was abolished when the hRFC-C/453 fragment was cloned into the antisense orientation (results not shown).

Potential transcription elements identified within the active 453 bp fragment are shown in Figure 8. Although neither a highly conserved TATA box nor Inr element was identified by database (i.e. Transfac; [39]) analysis, a number of potential conserved elements including GATA, Ikaros, GC box, E boxes, nuclear factor-1 ('NF-1') and CRE were identified (Figure 8).

243526

...GCCCCAGACATCACTGTATATGGCTGGAGC  
**Ikaros**  
 CTACAGGCTGGAGGGCCGGGATCCACTGCT

GGGCCCTGCTGATCCCTCCAACCCAGGGCTT  
**Ikaros**  
 CTCCAGGGACCAGCTCTCCCTGCCATCCCTGA  
**GATA**  
 CGCTCAGGCACTTAACTATTTGACAAACCGATA  
**MZF1**  
 ATGAAACACGCAAGGACGGGGACCGCTGGAGG  
**E-box**  
 CTCGTGAGGGCCCAAGCACAGGATCCATTCCC  
**AP1/Cre**  
 AGATGCCAGTGTCACTCCCAAGTCACCTGCGTT

TGTAAGTCTCTATTTGGGTGGAGCCCTCTGGA  
**GC-box**  
 AGCCCACGCCCCACTGTCTGTGGCCACTCCTCG

CAGTCCTCAATGGAGGTTTCTGTAAGTTCTTCA  
**E-box**  
 CGAGTCTCCTGGCTCTCCCTCAGAGCAGCTGC  
**NF1**  
 CTCTAGATTACAAGTCCCAAGTGTGTTGGTGG

243074

CAGAAGCCCTACCTCCCCACTCCGAAGCAG...

**Figure 8** Nucleotide sequence for the 453 bp promoter C region

The nucleotide sequence for the 453 bp promoter C region identified by reporter gene assays is shown in the sense direction, and the numbering corresponds to that for contig HS21C102. Potential *cis* elements that could be regulating promoter C are underlined and labelled with the transcription factor family type. Non-coding exon C sequence is given in italics.

## DISCUSSION

Folates are essential for cell survival because these derivatives participate in one-carbon transfer reactions, leading to the biosynthesis of purine nucleotides, thymidylate, serine and methionine [1]. Adequate rates of intracellular delivery of active tetrahydrofolate cofactors are important for DNA synthesis and cell proliferation. In mammalian cells, RFC is the primary route for the cellular uptake of reduced folates and antifolates [12–16]. Based on hRFC expression patterns in human tissues, RFC appears to participate in certain specialized transport functions, including absorption in intestine across the luminal epithelial cells [40,41], transplacental transport of folates [42], retinal epithelium transport of folates [43] and transport across the basolateral membrane of renal proximal tubule cells [44]. Decreased RFC expression in human tissues may contribute to disease states associated with reduced accumulation of folate cofactors and thus, may exacerbate the effects of folate deficiencies in relation to a variety of health-related problems, ranging from foetal abnormalities [3–7] to cardiovascular disease [2] and cancer [9–11]. Consistent with the critical role played by RFC in foetal development, an mRFC gene knock-out results in embryonic death if folic acid supplements are not provided [45]. Moreover, the mice that survived in the presence of folate supplements were smaller and showed marked decreases in haematopoiesis in bone marrow, spleen and liver [45].

The present study was undertaken to understand better the role of RFC in tissue physiology, by characterizing the gene

expression patterns for this essential transport system in human tissues. Our MTE array and MTN blotting results demonstrate that the hRFC gene is ubiquitously expressed in human tissues; however, the range of hRFC gene expression was broad. For adult tissues, the highest levels of hRFC were detected in placenta, suggesting a role for hRFC in transplacental transport of reduced folates. Considerable hRFC was also detected in liver, leucocytes, kidney, lung, bone marrow and parts of the intestine (i.e. highest in duodenum), as well as regions of the central nervous system and brain, whereas low but detectable hRFC was seen in the heart and skeletal muscle. Qualitatively similar results were previously reported for a human MTN blot probed with hRFC cDNA [40], for RT-PCR analysis of human tissue RNAs [31] and by immunohistochemistry of selected mouse tissues with an mRFC antibody [27]. In our analysis, a wide differential expression of hRFC was also observed in foetal tissues, with the highest levels in foetal lung and the lowest in heart.

These patterns of hRFC expression probably reflect tissue requirements for reduced folates or specialized tissue functions involving reduced folate cofactors and may, in part, relate to the pathophysiology of folate deficiencies. Moreover, patterns of hRFC expression may determine the anti-tumour activities of antifolates and contribute to tissue toxicities associated with antifolate chemotherapy. For example, hepatotoxicity can occur in patients receiving high doses of Mtx or frequent administration of low doses of Mtx [46,47]. Other toxicities associated with Mtx administration include pulmonary fibrosis, mucositis, bone marrow toxicities and leucoencephalopathy [46–48]. Although the detailed molecular mechanisms responsible for these untoward toxicities are not completely understood, in some cases, the patterns of hRFC expression in these tissues are consistent with a causal role.

The hRFC gene is regulated by two functional GC-rich, TATA-less promoters, designated hRFC-B and -A, each transcribing a unique non-coding exon (exons B and A respectively). Our previous studies identified key transcription factors that play important roles in regulating hRFC expression from the minimal hRFC-B and -A promoters, including the Sp family of proteins (for promoter B) and the basic leucine zipper DNA-binding proteins (for promoter A) [32]. Cell-specific expression of hRFC may involve differential levels of particular family members or alternate signalling pathways that influence the activity of various transcription factors. The levels of hRFC transcripts ultimately achieved within tissues probably reflect combinations of transcription factors that respond to specific stimuli and activate or repress transcription to ensure sufficient levels of folate uptake for cell proliferation and tissue regeneration.

A major goal of the present study was to understand the patterns of hRFC expression in assorted tissues and cell lines in terms of promoter and non-coding exon usage. Accordingly, we used 5'-RACE to identify the 5'-UTRs in hRFC transcripts from nine human tissues and two cell lines and, by extension, the hRFC promoters. The location of each non-coding exon, in relation to the ATG start site, was determined by aligning the 5'-RACE products to chromosome 21 contig HS21C102 and was confirmed by RT-PCR and primer extension. Altogether, we identified seven different hRFC non-coding exons that span approx. 35 kb upstream of the translation start. Four of the 5'-UTRs were characterized by multiple start sites and alternative splice forms. The net result was at least 18 potential hRFC transcripts with unique 5'-UTRs fused to the same open reading frame that, presumably, encode the same hRFC protein.

5'-UTR usage by 5'-RACE appeared to be tissue-specific, since for the caudate nucleus, forms C and D were predominant,

whereas B and A1 were the major forms identified from heart. An assortment of other samples showed exon B sequence, including liver, heart, bone marrow and placenta, as well as HepG2 cells. However, exon A2 was only observed in transcripts from adult liver. Although most of the putative 5'-UTR splice forms were detected in 5'-RACE clones from more than one tissue, tissue-specific splice patterns were, nonetheless, observed. Qualitative differences in the apparent 5'-UTRs and splice forms were also detected between foetal and adult tissues, implying that 5'-UTR splice forms may switch during foetal development and/or tissue maturation. Patterns of 5'-UTR utilization in human tissues were confirmed by RT-PCR.

The alternate non-coding exons were also observed for a variety of leukaemia and lymphoma cell lines. The UTRs were identical with the forms identified in normal tissues. Of particular interest were our results with K562.4CF cells, a K562 subline selected for growth in low levels of reduced folates and which expressed elevated levels of hRFC over parental K562 cells [33,38]. Increased hRFC transcripts in K562.4CF cells were accompanied by an apparent increase in all the 5'-UTRs when compared with parental K562 cells. The exact function of the large number of different hRFC mRNAs identified in the present study has not been determined. However, by analogy with other genes [49–57], these transcripts may be associated with altered translation efficiencies [49,55,56], mRNA stabilities [56,57], intracellular targeting [51,52] or even the synthesis of alternate proteins [53]. Studies are in progress to explore these possibilities.

Previous reports identified up to three non-coding exons for hRFC, corresponding to exons A, B and C [28–31]. However, none of these earlier studies identified hRFC exons A1, A2, D or E. Based on the analogy with other multi-promoter genes, the unique non-coding exons for hRFC are likely to be transcribed from distinct promoters. Whereas promoter activity is well established for promoters A and B [28,29,31,32], activity was not previously detected for the exon C 5'-flanking region [31].

Based on the detection of hRFC transcripts with exon C sequence in HepG2 cells, a 2883 bp fragment, containing the 580 bp exon C and 5'- and 3'-flanking regions, was subcloned into a pGL3-Basic reporter vector and transfected into HepG2 cells. Following the 3'-deletion of a 346 bp repressor region, promoter activity was detected and was localized to a 453 bp fragment, including 11 bp of exon C. A number of potential transcriptional elements were identified within this region, including GATA, Ikaros, GC box, nuclear factor-1, CRE-binding proteins and MZF-1. Studies are in progress to characterize further the functional elements in this putative tissue-specific promoter. Since the 346 bp repressor may explain the infrequent use of this exon/promoter C in assorted tissues and cell lines, including the absence of promoter activity in a previous study [31], we are also characterizing potential *cis* elements in this region.

In conclusion, our studies demonstrate that the hRFC gene is ubiquitously and differentially expressed in normal human tissues. Our results demonstrate that hRFC transcription involves up to seven unique non-coding exons, four of which exhibit multiple transcriptional starts and/or alternative splicing. Whereas our previous and present experiments confirm high levels of promoter activity for promoters A, B and C, the characterization of putative A1, A2, D and E promoters will undoubtedly require the identification of suitable cell culture models that utilize these 5'-UTRs/promoters. These studies are currently in progress. Another important unresolved question involves the significance of the diverse 5'-UTRs in relation to post-transcriptional effects on cellular folate homeostasis and antifolate drug selectivity during cancer chemotherapy.

This study was supported by grant no. CA53535 from the National Cancer Institute, National Institutes of Health (Bethesda, MD, U.S.A.).

## REFERENCES

- Stokstad, E. L. R. (1990) Historical perspective on key advances in the biochemistry and physiology of folates. In *Folic Acid Metabolism in Health and Disease* (Picciano, M. F., Stokstad, E. L. R. and Gregory, J. F., eds.), pp. 1–21. Wiley-Liss, New York
- Refsum, H., Ueland, P., Nygard, O. and Vollset, S. E. (1998) Homocysteine and cardiovascular disease. *Annu. Rev. Med.* **49**, 31–62
- Butterworth, Jr, C. E. and Bendich, A. (1996) Folic acid and the prevention of birth defects. *Annu. Rev. Nutr.* **16**, 73–97
- Hernandez-Diaz, S., Werler, M. M., Walker, A. M. and Mitchell, A. A. (2000) Folic acid antagonists during pregnancy and the risk of birth defects. *N. Engl. J. Med.* **343**, 1608–1614
- MRC Vitamin Study Research Group (1991) Prevention of neural tube defects: results of the Medical Research Council Vitamin Study. *Lancet* **327**, 131–137
- Berry, R. J., Li, Z., Erickson, J. D., Li, S., Moore, C. A., Wang, H., Mulinare, J., Zhao, P., Wong, L.-Y., Gindler, J. et al. (1999) Prevention of neural-tube defects with folic acid in China. *N. Engl. J. Med.* **341**, 1485–1490
- Honein, M. A., Paulozzi, L. J., Mathews, T. J., Erickson, J. D. and Wong, L.-Y. (2001) Impact of folic acid fortification of the US food supply on the occurrence of neural tube defects. *JAMA, J. Am. Med. Assoc.* **285**, 2981–2986
- Serot, J. M., Christmann, D., Dubost, T., Bene, M. C. and Faure, G. C. (2001) CSF-folate levels are decreased in late-onset AD patients. *J. Neural Transm.* **108**, 93–99
- Albanes, D. and Glynn, S. A. (1994) Folate and cancer: a review of the literature. *Nutr. Cancer* **22**, 101–119
- Kim, Y. I. J. (1999) Folate and carcinogenesis: evidence, mechanisms and implications. *J. Nutr. Biochem.* **10**, 66–88
- Choi, S.-W. and Mason, J. B. (2000) Folate and carcinogenesis: an integrated scheme. *J. Nutr.* **130**, 129–132
- Sirotnak, F. M. and Tolner, B. (1999) Carrier mediated membrane transport of folates in mammalian cells. *Annu. Rev. Nutr.* **19**, 91–122
- Matherly, L. H. (2001) Molecular and cellular biology of the human reduced folate carrier. *Prog. Nucleic Acid Res. Mol. Biol.* **67**, 131–162
- Goldman, I. D. and Matherly, L. H. (1985) The cellular pharmacology of methotrexate. *Pharmacol. Ther.* **28**, 77–100
- Jansen, G. (1999) Receptor- and carrier-mediated transport systems for folates and antifolates. Exploitation for folate chemotherapy and immunotherapy. In *Anticancer Development Guide: Antifolate Drugs in Cancer Therapy* (Jackman, A. L., ed.), pp. 293–321. Humana Press, Totowa, NJ
- Sirotnak, F. M. (1985) Obligate genetic expression in tumor cells of a fetal membrane property mediating 'folate' transport: biological significance and implications for improved therapy of human cancer. *Cancer Res.* **45**, 3992–4000
- Matherly, L. H. and Taub, J. W. (1996) Methotrexate pharmacology and resistance in childhood acute lymphoblastic leukemia. *Leuk. Lymphoma* **21**, 359–368
- Guo, W., Healey, J. H., Meyers, P. A., Ladanyai, M., Huvos, A. G., Bertino, J. R. and Gorlick, R. (1999) Mechanisms of methotrexate resistance in osteosarcoma. *Clin. Cancer Res.* **5**, 621–627
- Schuetz, J. D., Matherly, L. H., Westin, E. H. and Goldman, I. D. (1988) Evidence for a functional defect in the translocation of the methotrexate transport carrier in a methotrexate resistant murine L1210 leukemia cell line. *J. Biol. Chem.* **263**, 9840–9847
- Wong, S. C., McQuade, R., Proefke, S. A. and Matherly, L. H. (1997) Human K562 transfectants expressing high levels of reduced folate carrier but exhibiting low transport activity. *Biochem. Pharmacol.* **53**, 199–206
- Jansen, G., Mauritz, R., Drori, S., Sprecher, H., Kathman, I., Bunni, M., Priest, D. G., Noordhuis, P., Schornagel, J. H., Pinedo, H. M. et al. (1998) A structurally altered human reduced folate carrier with increased folic acid transport mediates a novel mechanism of antifolate resistance. *J. Biol. Chem.* **273**, 30189–30198
- Gong, M., Yess, J., Connolly, T., Ivy, S. P., Ohnuma, T., Cowan, K. H. and Moscow, J. A. (1997) Molecular mechanism of antifolate transport deficiency in a methotrexate resistant MOLT-3 human leukemia cell line. *Blood* **89**, 2494–2499
- Sadlish, H., Murray, R. C., Williams, F. M. R. and Flintoff, W. F. (2000) Mutations in the reduced folate carrier affect protein localization and stability. *Biochem. J.* **346**, 509–516
- Sirotnak, F. M., Moccio, D. M., Kelleher, L. E. and Goutas, L. J. (1981) Relative frequency and kinetic properties of transport-defective phenotypes among methotrexate resistant L1210 clonal cell lines derived *in vivo*. *Cancer Res.* **41**, 4442–4452
- Zhang, L., Taub, J. W., Williamson, M., Wong, S. C., Hukku, B., Pullen, J., Ravindranath, Y. and Matherly, L. H. (1998) Reduced folate carrier gene expression in childhood acute lymphoblastic leukemia: relationship to immunophenotype and ploidy. *Clin. Cancer Res.* **4**, 2169–2177

- 26 Gorlick, R., Goker, E., Trippett, T., Steinherz, P., Elisseyeff, Y., Mazumdar, M., Flintoff, W. F. and Bertino, J. R. (1997) Defective transport is a common mechanism of acquired methotrexate resistance in acute lymphoblastic leukemia and is associated with decreased reduced folate carrier expression. *Blood* **89**, 1013–1018
- 27 Wang, Y., Zhao, R., Russell, R. G. and Goldman, I. D. (2001) Localization of the murine reduced folate carrier as assessed by immunohistochemical analysis. *Biochim. Biophys. Acta* **1513**, 49–54
- 28 Zhang, L., Wong, S. C. and Matherly, L. H. (1998) Transcript heterogeneity of the human reduced folate carrier results from the use of multiple promoters and variable splicing of alternative upstream exons. *Biochem. J.* **332**, 773–780
- 29 Tolner, B., Roy, K. and Sirotnak, F. M. (1998) Structural analysis of the human RFC-1 gene encoding a folate transporter reveals multiple promoters and alternatively spliced transcripts with 5' end heterogeneity. *Gene* **211**, 331–341
- 30 Williams, F. M. and Flintoff, W. F. (1998) Structural organization of the human reduced folate carrier gene: evidence for 5' heterogeneity in lymphoblast mRNA. *Somat. Cell Mol. Genet.* **24**, 143–156
- 31 Gong, M., Cowan, K. H., Gudas, J. and Moscow, J. A. (1999) Isolation and characterization of genomic sequences involved in the regulation of the human reduced folate carrier gene (RFC1). *Gene* **233**, 21–31
- 32 Whetstine, J. R. and Matherly, L. H. (2001) The basal promoters for the human reduced folate carrier gene are regulated by a GC-box and a cAMP-response element/AP-1-like element. *J. Biol. Chem.* **276**, 6350–6358
- 33 Matherly, L. H., Czajkowski, C. A. and Angeles, S. M. (1991) Identification of a highly glycosylated methotrexate membrane carrier in K562 human erythroleukemia cells up-regulated for tetrahydrofolate cofactor and methotrexate transport. *Cancer Res.* **51**, 3420–3426
- 34 Sirotnak, F. M., Moccio, D. M. and Yang, C.-H. (1984) A novel class of genetic variants of the L1210 cell up-regulated for folate analogue transport inward. Isolation, characterization, and degree of metabolic instability of the system. *J. Biol. Chem.* **259**, 13139–13144
- 35 Yang, C.-H., Sirotnak, F. M. and Mines, L. S. (1988) Further studies on a novel class of genetic variants of the L1210 cell with increased folate analogue transport inward. Transport properties of a new variant, evidence for increased levels of a specific transport protein, and its partial characterization following affinity labeling. *J. Biol. Chem.* **263**, 9703–9709
- 36 Jansen, G., Westerhof, G. R., Jarmuszewski, M. J., Kathman, I., Rijksen, G. and Schornagel, J. H. (1990) Methotrexate transport in variant human CCRF-CEM leukemia cells with elevated levels of the reduced folate carrier. Selective effect on carrier-mediated transport of physiological concentrations of reduced folates. *J. Biol. Chem.* **265**, 18272–18277
- 37 Wong, S. C., Proefke, S. A., Bhushan, A. and Matherly, L. H. (1995) Isolation of human cDNAs that restore methotrexate sensitivity and reduced folate carrier activity in methotrexate transport-defective Chinese hamster ovary cells. *J. Biol. Chem.* **270**, 17468–17475
- 38 Wong, S. C., Zhang, L., Proefke, S. A., Hukku, B. and Matherly, L. H. (1998) Gene amplification and increased expression of the reduced folate carrier in transport elevated K562 cells. *Biochem. Pharmacol.* **55**, 1135–1138
- 39 Quandt, K., Frech, K., Karas, H., Wingender, E. and Werner, T. (1995) MatInd and MatInspector – new fast and versatile tools for detection of consensus matches in nucleotide sequence data. *Nucleic Acids Res.* **23**, 4878–4884
- 40 Nguyen, T. T., Dyer, D. L., Dunning, D. D., Rubin, S. A., Grant, K. E. and Said, H. M. (1997) Human intestinal folate transport. Cloning expression and distribution of complementary RNA. *Gastroenterology* **112**, 783–791
- 41 Chiao, J. H., Roy, K., Tolner, B., Yang, C.-H. and Sirotnak, F. M. (1997) RFC-1 gene expression regulates folate absorption in mouse small intestine. *J. Biol. Chem.* **272**, 11165–11170
- 42 Prasad, P. D., Ramamoorthy, S., Leibach, F. H. and Ganapathy, V. (1995) Molecular cloning of the human placental folate transporter. *Biochem. Biophys. Res. Commun.* **206**, 681–687
- 43 Chancy, C. D., Kekuda, R., Huang, W., Prasad, P. D., Kuhnel, J.-M., Sirotnak, F. M., Roon, P., Ganapathy, V. and Smith, S. B. (2000) Expression and differential polarization of the reduced-folate transporter-1 and the folate receptor  $\alpha$  in mammalian retinal pigment epithelium. *J. Biol. Chem.* **275**, 20676–20684
- 44 Morshed, K. M., Ros, D. M. and McMartin, K. E. (1997) Folate transport proteins mediate the bidirectional transport of 5-methyltetrahydrofolate in cultured human proximal tubule cells. *J. Nutr.* **127**, 1137–1147
- 45 Zhao, R., Russell, R. G., Wang, Y., Liu, L., Gao, F., Kneitz, B., Edelman, W. and Goldman, I. D. (2001) Rescue of embryonic lethality in reduced folate carrier-deficient mice by maternal folic acid supplementation reveals early neonatal failure of hematopoietic organs. *J. Biol. Chem.* **276**, 10224–10228
- 46 Perry, M. C. (ed.) (1992) *The Chemotherapy Source Book*, Williams and Wilkins, Baltimore, MD
- 47 Dorr, R. T. and Von Hoff, D. D. (eds.) (1994) *Cancer Chemotherapy Handbook*, 2nd edn, Appleton and Lange, Norwalk, CT
- 48 Filley, C. M. and Kleinschmidt-Demasters, B. K. (2001) Toxic leukoencephalopathy. *N. Engl. J. Med.* **345**, 425–432
- 49 Roberts, S. J., Chung, K.-N., Nachmanoff, K. and Elwood, P. C. (1997) Tissue-specific promoters of the  $\alpha$  human folate receptor gene yield transcripts with divergent 5' leader sequences and different translational efficiencies. *Biochem. J.* **326**, 439–447
- 50 Elwood, P. C., Nachmanoff, K., Saikawa, Y., Page, S. T., Pacheco, P., Roberts, S. and Chung, K.-N. (1997) The divergent 5' termini of the  $\alpha$  human folate receptor (hFR) mRNAs originate from two tissue-specific promoters and alternative splicing: characterization of the  $\alpha$  hFR gene structure. *Biochemistry* **36**, 1467–1478
- 51 Chen, L., Qi, H., Korneberg, J., Garrow, T. A., Choi, Y.-J. and Shane, B. (1996) Purification and properties of human cytosolic folylpoly- $\gamma$ -glutamate synthetase and organization, localization, and differential splicing of its gene. *J. Biol. Chem.* **271**, 13077–13087
- 52 Roy, K., Mitsugi, K. and Sirotnak, F. M. (1996) Organization and alternate splicing of the murine folylpolyglutamate synthetase gene. *J. Biol. Chem.* **271**, 23820–23827
- 53 Turner, F. B., Andreassi, I., J. L., Ferguson, J., Titus, S., Tse, A., Taylor, S. M. and Moran, R. G. (1999) Tissue-specific expression of functional isoforms of mouse folylpoly- $\gamma$ -glutamate synthetase: a basis for targeting folate antimetabolites. *Cancer Res.* **59**, 6074–6079
- 54 Turner, F. B., Taylor, S. M. and Moran, R. G. (2000) Expression patterns of the multiple transcripts from the folylpolyglutamate synthetase gene in human leukemias and normal differentiated tissues. *J. Biol. Chem.* **275**, 35960–35968
- 55 Kocarek, T. A., Zangar, R. C. and Novak, R. F. (2000) Post-transcriptional regulation of rat CYP2E1 expression: role of CYP2E1 mRNA untranslated regions in control of translational efficiency and message stability. *Arch. Biochem. Biophys.* **376**, 180–190
- 56 Fiaschi, T., Chiarugi, P., Veggi, D., Raugel, G. and Ramponi, G. (2000) The inhibitory effect of the 5' untranslated region of muscle acylphosphatase mRNA on protein expression is relieved during cell differentiation. *FEBS Lett.* **473**, 42–46
- 57 Fournier, B., Trunong-Bolduc, Q. C., Zhang, X. and Hooper, D. C. (2001) A mutation in the 5' untranslated region increases stability of *norA* mRNA, encoding a multidrug resistance transporter of *Staphylococcus aureus*. *J. Bacteriol.* **183**, 2367–2371

Received 2 April 2002/28 June 2002; accepted 29 July 2002

Published as BJ Immediate Publication 29 July 2002, DOI 10.1042/BJ20020512